Optical wavelength conversion by cross-phase modulation of data signals up to 640 Gb/s

Galili, Michael; Oxenløwe, Leif Katsuo; Mulvad, Hans Christian Hansen; Clausen, Anders; Jeppesen, Palle

Published in:
I E E E Journal on Selected Topics in Quantum Electronics

Link to article, DOI:
10.1109/JSTQE.2008.915527

Publication date:
2008

Document Version
Publisher's PDF, also known as Version of record

Optical Wavelength Conversion by Cross-Phase Modulation of Data Signals up to 640 Gb/s

Michael Galili, Leif Katsuo Oxenløwe, Hans Christian Hansen Mulvad, Anders Thomas Clausen, and Palle Jeppesen, *Member, IEEE*

***Abstract*—In this paper, all-optical wavelength conversion by cross-phase modulation in a highly nonlinear fiber is investigated. Regenerative properties of the wavelength converter are demonstrated, and the effect of adding Raman gain to enhance the performance of the wavelength converter is shown. The wavelength conversion scheme is demonstrated at the record-high bit rate of 640 Gb/s.**

***Index Terms*—Nonlinear signal processing, optical time-division multiplexing, wavelength conversion.**

I. Introduction

THE SINGLE-CHANNEL bit rate has continuously increased in optical transmission systems and networks, reaching 10–40 Gb/s in deployed systems. To promote the increase in single-channel bit rates, schemes for appropriate signal processing need to be developed. At very high bit rates, all-optical signal processing has great potential for low penalty operation combined with an increased transparency in the optical network compared to current technologies. The wavelength conversion of data signals is a key signal processing task to be addressed in any optical network. At the present time, two schemes have been demonstrated for wavelength conversion of data signals up to 320 Gb/s. One scheme is based on the conversion in a semiconductor optical amplifier (SOA), and relies on a filtered chirp and the interaction of cross-phase modulation (XPM) and cross-gain modulation for generating the wavelength-converted signal. This scheme has been demonstrated at 320 Gb/s in [1]. A similar scheme relies on a filtering XPM-induced chirp generated in a nonlinear optical fiber. This was originally proposed by Olsson *et al*. [2]. The XPM conversion of a 40 Gb/s optical time-division multiplexing (OTDM) signal was performed with ∼1 dB penalty in the receiver sensitivity in [3], while the conversion of a strongly degraded 80 Gb/s signal produced ∼2 dB sensitivity improvement, demonstrating signal regeneration. The XPM conversion has been demonstrated at 320 Gb/s with virtually penalty-free performance (0.2 dB penalty in receiver sensitivity) in [4].

Manuscript received November 1, 2007; revised December 20, 2007. This work was supported in part by the Danish Research Council under the Programkomitéen for Nanovidenskab og -teknologi, Bioteknologi og IT (NABIIT) framework as part of the Project *UltraNet*.

The authors are with the Department of Communications Optics and Materials (COM·DTU), Technical University of Denmark, Lyngby, DK-2800, Denmark (e-mail: mg@com.dtu.dk; lo@com.dtu.dk; hchm@com.dtu.dk; atc@com.dtu.dk; pj@com.dtu.dk).

Color versions of one or more of the figures in this paper are available online at http://ieeexplore.ieee.org.

Digital Object Identifier 10.1109/JSTQE.2008.915527

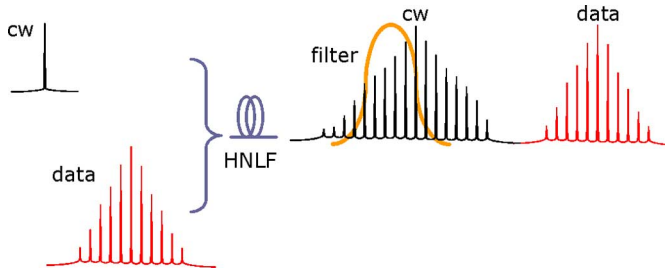

Fig. 1. Operating principle of XPM-based wavelength conversion.

In this paper, the wavelength conversion based on Raman-assisted XPM in a highly nonlinear fiber (HNLF) is investigated. Regenerative properties are demonstrated with sensitivity improvements up to 4.8 dB for degraded input data signals. The effect of adding Raman gain to the conversion process is illustrated, and sensitivity improvements up to 2.4 dB are recorded. Finally, the XPM wavelength converter is demonstrated for error-free conversion of a 640 Gb/s OTDM data signal [5]. This constitutes the highest operating speed of a wavelength converter to date.

II. Wavelength Conversion by XPM

A. Principle of Conversion

The operating principle of the XPM wavelength conversion is illustrated in Fig. 1.

A data signal and a continuous wave (CW) probe are launched together into a nonlinear medium, in this case an HNLF. The data signal is amplified to achieve sufficient peak power in the data marks to cause XPM in the fiber. The XPM will act to broaden the spectrum of the CW probe, where a mark has copropagated with it through the fiber. In this way, spectral sidebands are generated on the probe signal through the modulation of the phase in the fiber. At the output of the HNLF, the sidebands on the CW probe can be extracted by spectral filtering, generating an amplitude-modulated signal from the phase modulation of the CW probe. This amplitude-modulated signal will thus form a wavelength-converted replica of the original data signal. The XPM phase shift of the probe is localized to the part of the probe that has copropagated with a strong pulse through the fiber. In this way, if the strong pulses represent an ON-OFF keying (OOK) data signal, the phase modulation of the probe will represent the same data logic as the original pulses. The setup for the XPM wavelength conversion using this scheme is sketched in Fig. 1.

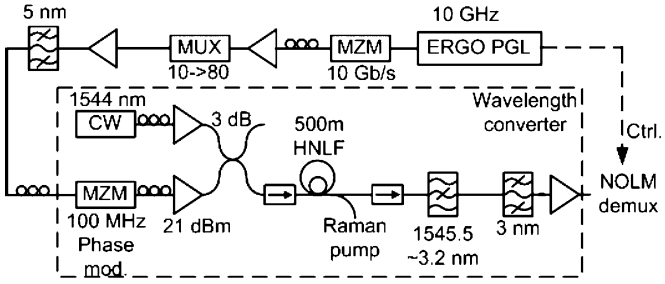

Fig. 2. Setup for 80 Gb/s characterization of the XPM wavelength conversion.

The data signal and the probe are combined at appropriate power levels, and injected into an HNLF. Here, the XPM generates red- and blue-shifted sidebands on the CW probe. One of these sidebands is extracted by using optical filtering. In order to extract as much power as possible from a sideband, a filter with a large bandwidth and a very steep edge is desirable to allow filtering close to the CW probe as described later.

A tradeoff exists between increasing the power in the converted signal and minimizing the CW probe present in the converted signal. To increase the converted signal power, a bandpass filter with a large bandwidth is desirable, as this will extract a larger fraction of the power available in the sideband, and allow for the extraction of narrow pulses. On the other hand, a strong suppression of the CW is required, as power at the CW probe wavelength will appear as a dc background level in the converted signal. Additionally, the sideband that will not be used as the wavelength-converted output must be suppressed. The two sidebands are temporally separated as they are chirp components formed by opposite slopes of a given data pulse, and therefore, to avoid pulse splitting, only one sideband must be present in the converted output signal [6].

B. Experimental Procedure

The experimental setup for implementing the XPM-based wavelength conversion is shown in Fig. 2.

The optical data signal is based on pulses generated by an erbium glass oscillator (ERGO) pulse source supplying a 10 GHz pulse train at a wavelength of 1557 nm with a pulsewidth of 2 ps full-width at half-maximum (FWHM). The pulse train is data modulated in a Mach–Zehnder modulator (MZM) encoding a $2^7 - 1$ pseudorandom bit sequence (PRBS) on the pulse train. The 10 Gb/s optical data signal is then multiplexed—in this case, only to 80 Gb/s for characterization purposes—in a passive fiber delay multiplexer (MUX). The MUX is polarization maintaining for increased stability and to ensure a truly single-polarization state of the signal. At a pattern length of $2^7 - 1$, the MUX is a PRBS maintaining meaning that the output of the MUX will have the same PRBS data logic as the input 10 Gb/s signal. This is the case regardless of the chosen output bit rate from the MUX up to 640 Gb/s. The phase modulation of the multiplexed data signal is performed by a symmetrically driven MZM at 100 MHz to ensure that narrow spectral components of the multiplexed high-speed signal do not initiate stimulated brillouin scattering (SBS) in the HNLF [6], [7]. The signal is amplified by an erbium-doped fiber amplifier (EDFA) to $\sim$21 dBm and combined with a CW probe before it is injected into the HNLF. The CW probe is amplified to 14.6 dBm before the signals are combined. In order to reduce SBS in the HNLF, the linewidth of the probe has been broadened to $\sim$500 MHz by introducing a weak frequency modulation in the CW laser source. The two signals are launched into 500 m of HNLF that has a nonlinear coefficient of $\sim 10\ \mathrm{W}^{-1}\cdot\mathrm{km}^{-1}$. The zero dispersion is at $\lambda_0 = 1551$ nm, and the fiber has a very flat dispersion profile with a slope of $0.017\ \mathrm{ps/nm}^2\cdot\mathrm{km}$. The limitations on the wavelength allocation of the data signal and the CW probe in the HNLF are strongly dependent on the fiber parameters, and on the target bit rate of the wavelength converter determining the allowable pulse broadening during conversion. Three considerations apply to the wavelength allocation. First, placing the original data signal and the CW probe symmetrically around λ_0 minimizes the pulse broadening due to dispersive walk-off between the two signals during conversion. Second, placing the original data signal close to λ_0 reduces dispersion-induced pulse broadening of the original data pulses, which also affects the wavelength-converted output. Finally, the minimum wavelength separation between the two signals in the HNLF is determined by the spectral width of the original data signal. Overlap between the original data signal and the XPM sideband forming the converted output results in interference degrading the converted output signal. In this demonstration, the wavelengths of the CW probe and the data signal are placed nearly symmetrically around λ_0 to reduce the group-velocity-dispersion-induced walk-off between the two signals to $\sim$0.1 ps in the HNLF. The distance between the original signal and the CW probe is sufficient to accommodate the broad spectrum associated with the wavelength conversion of a high-bit-rate data signal. In Section IV, a very similar configuration is demonstrated for wavelength conversion at 640 Gb/s. At the output of the HNLF, a wavelength-selective coupler is used to couple a counterpropagating $\sim$650 mW Raman pump into the HNLF while letting the output signal pass with low loss ($\sim$1 dB). The blue-shifted XPM sideband generated on the CW probe is filtered out using a combination of a chirped fiber Bragg grating (FBG) and a 3-nm-bandwidth bandpass filter. The FBG is applied in the transmission configuration with the Bragg wavelengths reflected into an isolator, giving an almost rectangular-shaped notch filter. This notch filter is then used to suppress the CW probe and the red-shifted XPM sideband, while the bandpass filter suppresses the original data signal and the residual power in the red-shifted sideband.

The FBG has center wavelength at 1545.5 nm and a 3 dB bandwidth of $\sim$2 nm. After filtering, the wavelength-converted signal is amplified, and then, demultiplexed in a nonlinear optical loop mirror (NOLM) to the 10 Gb/s base rate. This is done by using 2 ps control pulses from the 10 GHz 1557 nm pulse source to generate XPM in the HNLF in the NOLM.

C. Effect of Gain During Conversion

The effect of applying the Raman pump during wavelength conversion is seen in Fig. 3. Adding Raman gain to the

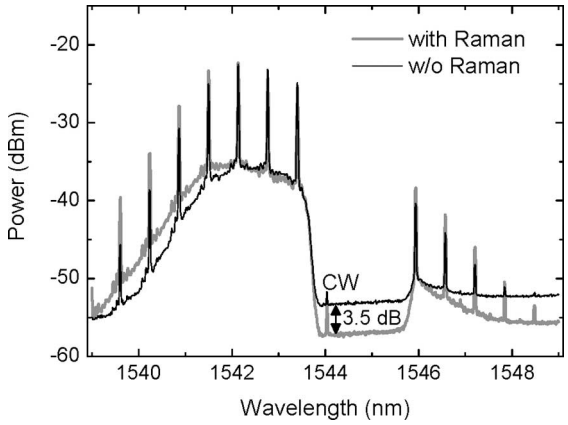

Fig. 3. Optical spectra for the wavelength-converted signal showing the effect of applying Raman gain to the conversion process.

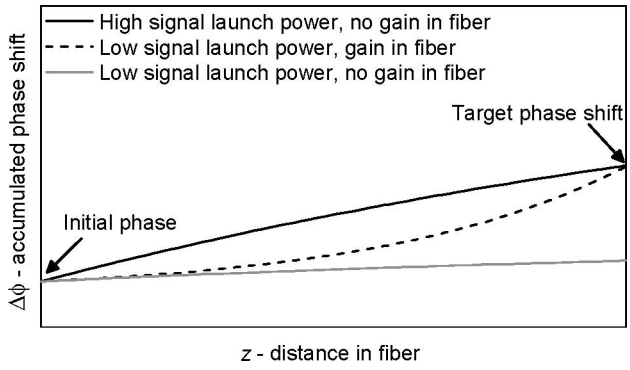

Fig. 4. Calculated accumulated phase shift by XPM in HNLF.

conversion process alters one of the features of the nonlinear interaction—namely that the power of the interacting signals decrease as they propagate through the HNLF. When Raman gain is present, the signals will grow stronger when propagating through the HNLF. In [3], this is described as an increase in the effective length (L_{eff}) of the interaction, increasing the accumulated phase shift for a given signal power level into the HNLF. The maximum accumulated phase shift at the output of the HNLF is then given by

$$\Delta\phi = \gamma P L_{\text{eff}} \tag{1}$$

where γ is the nonlinear coefficient of the fiber, P is the peak power of the optical pulse inducing XPM, and L_{eff} is the effective length of the interaction in the fiber. In the presence of both gain and loss processes in the fiber, L_{eff} becomes

$$L_{\text{eff}} = \frac{(1 - e^{(-\alpha+g)z})}{(\alpha - g)} \tag{2}$$

where α is the fiber loss while g is the gain in the fiber. The actual distance that the signals have traveled in the fiber is given by z.

To illustrate the effect of performing wavelength conversion in a fiber with gain, the two cases of wavelength conversion with and without gain are considered. When designing the XPM wavelength converter, it may be useful to target a given maximum accumulated phase shift ($\Delta\varphi$) of the CW probe at the output of the nonlinear fiber. The target phase shift is determined by the desired pulsewidth in the converted signal and by the applied filter configuration. In Fig. 4, the evolution of $\Delta\varphi$ through the fiber is illustrated by calculating $\Delta\varphi$ at different distances in the fiber.

Comparing the solid gray line and the dashed line in the figure, it is clear that, in order to achieve the targeted phase shift, it is necessary to apply a higher signal launch power when no gain is present in the fiber. The black line illustrates the phase shift achieved in the fiber with no gain, when the signal launch power is increased to reach the target phase shift at the fiber output. Increasing the nonlinear phase shift for a given launch power in this way may improve the optical signal to noise ratio (OSNR) of the converted output by allowing more efficient generation of XPM sidebands with less initial amplification of the original data signal. Additionally, if the CW probe is amplified while passing through the HNLF, more power will be available in the wavelength-converted output signal, for a given CW launch power. In this way, if the wavelength-converted output is stronger, less amplified spontaneous emission (ASE) noise will be generated when the converted signal is amplified at the output of the converter. This is seen in Fig. 3, where the noise level after filtering and amplification is lowered by 3.5 dB while the signal power is increased by $\sim$2 dB.

III. Regenerative Properties of XPM Conversion

After wavelength conversion, the signal is demultiplexed as described earlier, and the quality of the signal is evaluated by bit error rate (BER) measurements. Fig. 5 shows the BER results for wavelength conversion of an 80 Gb/s data signal.

The performance of the wavelength-converted and demultiplexed data signal is compared with the BER performance of the 10 Gb/s base rate signal. It is seen that the performance of the wavelength converter varies significantly, depending on the configuration of the wavelength converter, i.e., with and without the application of Raman gain. In Fig. 5(a), in the case of doing the wavelength conversion without the presence of Raman gain, the receiver sensitivity at BER 10^{-9} is $\sim$0.5 dB better than the 10 Gb/s reference. This improvement in sensitivity is attributed to the fact that the modulated 10 Gb/s signal has a small amount of unsuppressed optical power in the logic "0"s, which is also visible in the eye diagram of the corresponding original data signal. In the eye diagram of the converted signal, the "0" level noise is no longer visible.

This imperfect "0" level is suppressed in the wavelength conversion, as the transfer function for the XPM conversion is nonlinear having very weak transfer of low power levels in the input data signal [3]. Adding Raman gain to the conversion initially degrades the performance introducing 0.6 dB penalty compared to the 10 Gb/s reference. The optimum performance of the converter, when applying the Raman pump, is achieved by reducing the average power of the 80 Gb/s signal into the HNLF by $\sim$1 dB. This changes the performance drastically, resulting in a 1.6 dB improvement compared to the original 10 Gb/s signal. This illustrates the effect of the Raman pump to not only increase the power of the interacting signals, but also to

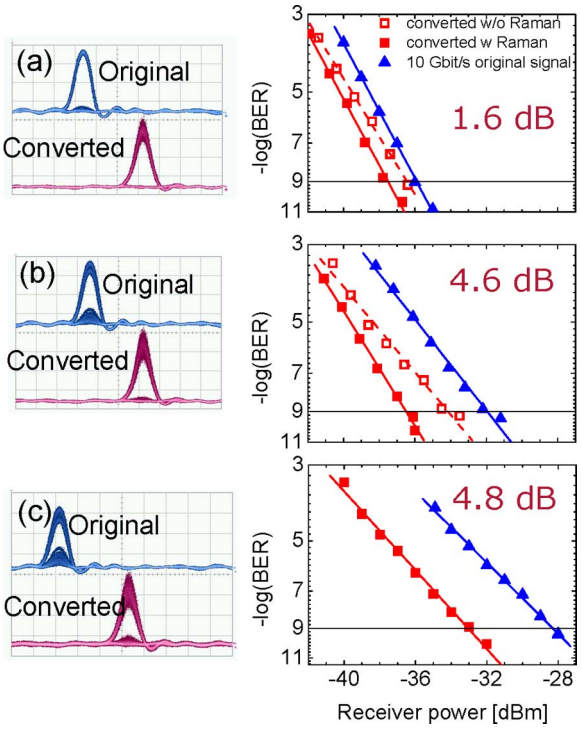

Fig. 5. Eye diagrams and BER performance of the XPM converter at 80 Gb/s for a degraded input signal. The BER results indicate the best performing channel (same channel throughout the characterization). Variation in receiver sensitivity among all channels is less than 0.5 dB. The XPM converter suppresses noise at the "0" level in the data signal resulting in a sensitivity improvement up to 4.8 dB after conversion compared to the original data signal. The sensitivity improvement for each configuration is indicated in dB in each BER curve.

alter the power profile of the signals passing through the HNLF by substituting the fiber loss with a net Raman gain. This lowers the input data power required to achieve a given accumulated phase shift, as indicated in Fig. 4. The observed regenerative effect of the wavelength conversion is further characterized in Fig. 5(b) and (c). Here, the input data signal has been deliberately degraded by altering the biasing of the MZM used for data modulation. This introduces noise in the "0" level and some in the "1" level, as seen in the eye diagrams. In Fig. 5(b), the 10 Gb/s reference suffers a penalty of 3.9 dB compared to the one in Fig. 5(a). Without Raman gain, the converted signal in Fig. 5(b) has a sensitivity improvement of ~2.2 dB compared to the original 10 Gb/s signal. However, adding Raman gain to the conversion and reducing the signal launch power, the sensitivity improvement increases to ~4.6 dB. Compared to the case in Fig. 5(a), the wavelength-converted signal has only suffered a 1 dB penalty from degrading the input signal 3.9 dB.

In Fig. 5(c), the input signal has been degraded even further as shown in the eye diagram in the figure. This imposes a penalty of ~7.6 dB on the original 10 Gb/s signal as compared to the case in Fig. 5(a). After Raman-assisted wavelength conversion and demultiplexing of the signal, the sensitivity is improved by 4.8 dB. It is seen that the improvement is virtually the same as for the previous case, indicating a saturation of the regenerative effect when the noise is increased beyond a certain level. Some residual noise is also seen in the "0" level of the wavelength-converted eye.

In the three configurations in Fig. 5, it is seen that the noise in the "1"-level of the signal is transferred and possibly increased by the conversion. An increase in noise in the "1"-levels can be explained by the same nonlinear transfer of the wavelength converter, which is responsible for suppressing noise in the "0"-level. It is, however, expected that a regenerative effect can be obtained for both "0"s and "1"s using this conversion scheme. This requires a stronger broadening of the CW probe, for a given filter configuration in the converter, compared to what is being used here.

IV. Wavelength Conversion of High-Speed Data

The XPM-based wavelength converter relies on the Kerr nonlinearity in optical fiber. As such, it is expected to have potential for a very-high-bit-rate operation due to the fast response time of the fiber nonlinearity—on the order of a few femtoseconds. This is demonstrated by using the potential of the OTDM technology, to achieve high-bit-rate single channel data signals up to 640 Gb/s.

A. Setup for 640 Gb/s XPM Conversion

The experimental setup for 640 Gb/s XPM wavelength conversion is shown in Fig. 6. The optical data signal at 1557 nm is generated, modulated, and multiplexed to 40 Gb/s in the same way as described previously. In order to achieve a bit rate of 640 Gb/s, it is, however, necessary to introduce nonlinear pulse compression in order to reduce the pulsewidth. This is done at 40 Gb/s in order to avoid having to transmit the narrow pulses through the first multiplexer stages comprising the longest dispersive fiber delay lines. In this way, the differential pulse broadening caused by the multiplexer is reduced. In the pulse compressor, the 40 Gb/s data pulses are chirped and spectrally broadened by self phase modulation (SPM) in 400 m of dispersion flattened highly nonlinear fiber (DF-HNLF, $\gamma \sim 10$ W^{-1} km^{-1}, dispersion $D = -1.2$ ps/(nm·km) at 1550 nm, and a dispersion slope of 0.003 ps/nm^2·km). The positive dispersion in the remainder of the transmitter linearly compresses the data pulses from ~2 ps to 560 fs FWHM. This occurs while the data signal is multiplexed further up to 640 Gb/s. The signal is amplified by an EDFA to ~28 dBm, and is combined with a ~25 dBm CW at 1544 nm before injection into 200 m of HNLF ($\gamma \sim 10$ W^{-1}·km^{-1}, zero dispersion at 1552 nm, and a dispersion slope of 0.018 ps/nm^2·km). The CW is frequency modulated in the source, as described earlier. An additional phase modulation is applied at 100 MHz to reduce the SBS. The increased linewidth combined with the shorter HNLF sample allows for this high-CW power to be launched into the HNLF without causing SBS. A counterpropagating 800 mW Raman pump enhances the wavelength conversion in the HNLF. The filtering scheme used to extract the wavelength-converted signal comprises an FBG notch filter and a 9 nm bandpass filter. The FBG has its center wavelength at 1545.5 nm, a bandwidth of 3.2 nm, and a suppression of ~40 dB. The wavelength-converted signal is demultiplexed to the 10 Gb/s base rate in a NOLM

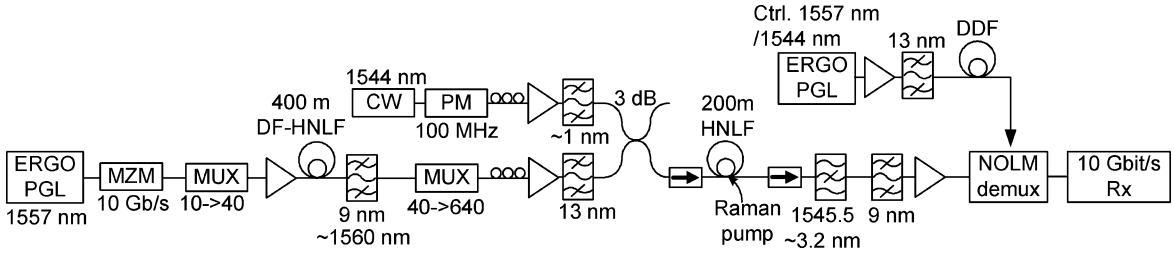

Fig. 6. Setup for 640 Gb/s XPM wavelength conversion.

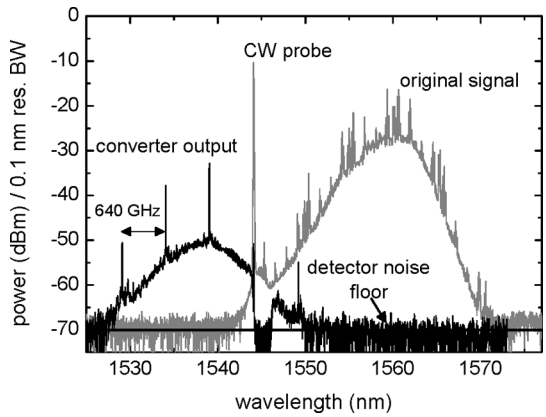

Fig. 7. Optical spectra illustrating the wavelength conversion process. The original signal along with the CW probe at the input to the HNLF is shown in the gray line. The output of the HNLF after filtering is shown in the black line. This is the spectrum of the wavelength-converted signal.

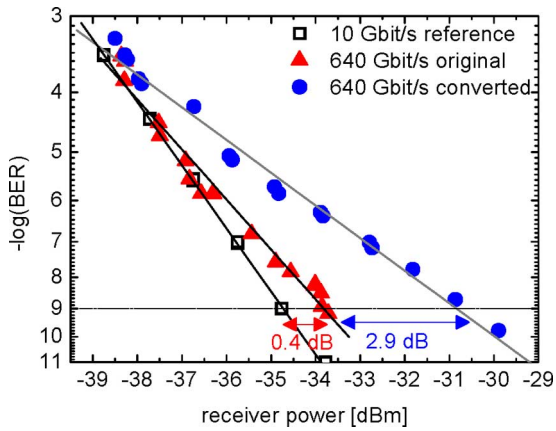

Fig. 8. BER measurements for the converted and original 640 Gb/s data signals.

using 780 fs control pulses generated by adiabatic soliton compression of a 10 GHz pulse train (from a second ERGO pulse source) in a dispersion decreasing fiber (DDF). BER measurements are performed to evaluate the system performance.

B. Experimental Results

Fig. 7 shows the optical spectrum of the wavelength-converted data signal after filtering at ~1539 nm as well as the original 640 Gb/s data signal and the CW probe at the input to the HNLF.

The converted spectrum contains strong modulation peaks spaced 640 GHz. These peaks are much more pronounced after the wavelength conversion as the converted signal has adopted the phase properties of the CW probe signal, giving a stable phase relationship between consecutive pulses in the wavelength-converted OTDM data signal [8]. In the original data signal, the modulation peaks are unstable and much less pronounced, since there is no stable phase relationship between consecutive pulses in the multiplexed OTDM data signal.

In the filtered output signal in Fig. 7, strong suppression of the CW probe is seen, which is mainly achieved by the use of the FBG notch filter. The original data signal and red-shifted CW sideband are also well suppressed in the converted output, indicating that the impairments caused by the presence of these

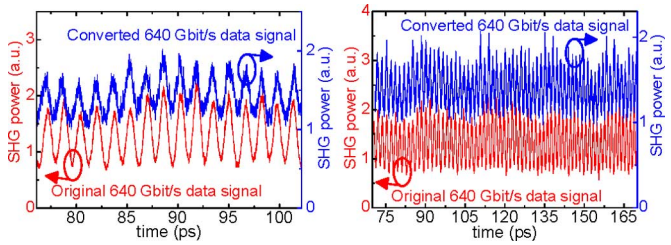

Fig. 9. Cross-correlations—lower traces, 640 Gb/s original data (FWHM ~560 fs). Upper traces, converted data (FWHM ~660 fs). Left, zoom in on 16 channels. Right, all 64 channels.

spectral components in the converted output has been strongly limited.

Fig. 8 shows BER results for the 640 Gb/s original data signal and for the wavelength-converted signal when demultiplexed down to 10 Gb/s. The 640 Gb/s wavelength conversion is successful with an error-free performance. For both the original and the converted 640 Gb/s signal, the error-free performance (defined as BER $< 10^{-9}$) with no sign of an error floor is obtained. In Fig. 8, a typical channel is shown for the original 640 Gb/s data signal (channel 64 in Fig. 10), whereas the BER curve for the converted 640 Gb/s signal corresponds to one of the best performing channels in the converted signal (channel 23 in Fig. 10), having a conversion penalty of only 2.9 dB.

Fig. 9 shows cross-correlations of the 640 Gb/s original data signal together with the converted 640 Gb/s signal.

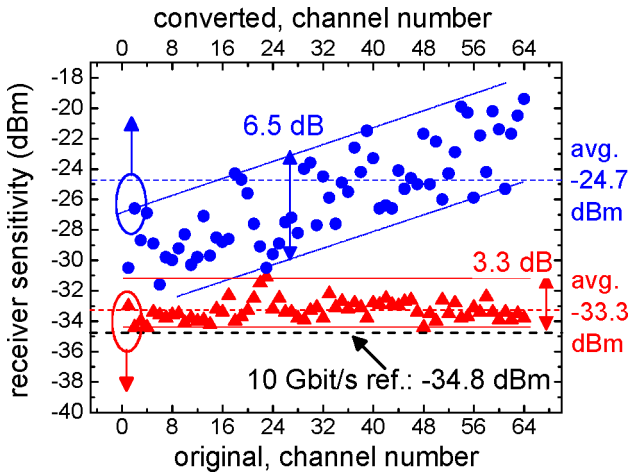

Fig. 10. Receiver sensitivity at a BER of 10^{-9} for all OTDM channels in the converted and original 640 Gb/s data signals.

The average pulsewidth of the two signals is measured on an autocorrelator to be ~560 fs before the conversion and 660 fs after the conversion. This increase in pulsewidth is seen to cause a reduction in contrast in the cross-correlations of the converted signal as compared to the original signal. The temporal resolution of the cross-correlations is partly limited by the width of the sampling pulse (~800 fs FWHM), meaning that the actual pulse overlap after the conversion is significantly less than that indicated by the traces in Fig. 9. There is an ~1 dB amplitude difference among the original data channels and among the converted channels. Subsequently, all 64 channels are demultiplexed and are subject to BER measurements.

Fig. 10 shows the measured receiver sensitivities (at BER = 10^{-9}) of all 64 channels in the converted and the original signals. All 64 converted channels achieve error-free operation, demonstrating successful wavelength conversion of the full 640 Gb/s data signal. The original OTDM signal has an average sensitivity of −33.3 dBm, i.e., an average penalty of only 1.5 dB compared to the 10 Gb/s reference measured at the output of the data modulation. The converted signal has a penalty of ~3 dB compared to the 10 Gb/s reference under optimized conditions. This penalty is mainly believed to be caused by the pulse broadening associated with the wavelength conversion. The pulse broadening is, in turn, caused by the filter configuration used to extract the output signal from the wavelength converter. There is a ~6.5 dB sensitivity spread due to channel variations in the wavelength-converted signal. The increased sensitivity to channel variations in the converted signal is expected to be mainly due to the pulse broadening during conversion. On top of this, an ambient drift affected the system for the duration of the measurement, resulting in a slowly deteriorating sensitivity, yielding an average receiver sensitivity of −24.7 dBm. A significantly more stable performance of the converter is thus expected, if the impact of ambient conditions can be reduced. Additionally, optimizing the filter configuration in the wavelength converter to further reduce pulse broadening is expected to improve the overall performance of the converter.

V. Conclusion

We have investigated the regenerative properties of the XPM-based wavelength conversion in an HNLF, and have observed significant signal reshaping capabilities resulting in sensitivity improvements up to 4.8 dB. Furthermore, we demonstrate the XPM-based wavelength conversion of a 640 Gb/s data signal. This constitutes the highest bit rate reported in a wavelength conversion demonstration to date. The wavelength conversion allows error-free operation of all tributary channels in the converted signal. The potential for low-penalty wavelength conversion, compared to the input signal, is demonstrated.

Acknowledgment

The authors would like to acknowledge OFS Fitel Denmark ApS for providing the highly nonlinear fibers (HNLFs) used in this paper. Furthermore, Tellabs Denmark is acknowledged for providing a Raman pump for the experiments.

References

[1] Y. Liu, E. Tangdiongga, Z. Li, H. de Waardt, A. M. J. Koonen, G. D. Khoe, H. J. S. Dorren, X. Shu, and I. Bennion, "Error-free 320 Gb/s SOA-based wavelength conversion using optical filtering," presented at the Tech. Dig. Opt. Fiber Commun. Conf., OFC'2006, Anaheim, CA., Mar.

[2] B.-E. Olsson, P. Öhlén, L. Rau, and D. J. Blumenthal, "A simple and robust 40-Gb/s wavelength converter using fiber cross-phase modulation and optical filtering," *IEEE Photon. Technol. Lett.*, vol. 12, no. 7, pp. 846–848, Jul. 2000.

[3] W. Wang, H. Poulsen, L. Rau, H. Chou, J. E. Bowers, and D. J. Blumenthal, "Raman-enhanced regenerative ultrafast all-optical fiber XPM wavelength converter," *J. Lightw. Technol.*, vol. 23, no. 3, pp. 1105–1115, Mar. 2005.

[4] M. Galili, H. C. H. Mulvad, L. K. Oxenløwe, A. T. Clausen, and P. Jeppesen, "Low-penalty Raman-assisted XPM wavelength conversion at 320 Gb/s," presented at the Tech. Dig. Conf. Lasers Electro-Opt., CLEO'2007, Baltimore, MD, May.

[5] M. Galili, H. C. Hansen Mulvad, L. K. Oxenløwe, H. Ji, A. T. Clausen, and P. Jeppesen, "640 Gbit/s wavelength conversion," presented at the Tech. Dig. Opt. Fiber Commun. Conf., OFC 2008, San Diego, CA, Feb.

[6] M. Galili, L. K. Oxenløwe, D. Zibar, A. Clausen, and P. Jeppesen, "Characterisation of systems for Raman-assisted high-speed wavelength conversion," in *Proc. Tech. Dig. Conf. Lasers Electro-Opt., CLEO'2005*, Baltimore, MD, May, pp. 288–290.

[7] T. Hirooka, K. Osawa, M. Okazaki, M. Nakazawa, and H. Murai, "Observation of stimulated Brillouin scattering in ultrahigh-speed in-phase and carrier-suppressed RZ OTDM transmission," presented at the Eur. Conf. Opt. Commun., ECOC'2007, Berlin, Germany, Sep.

[8] L. Rau, W. Wang, S. Camatel, H. Poulsen, and D. J. Blumenthal, "All-optical 160-Gb/s phase reconstructing wavelength conversion using cross-phase modulation (XPM) in dispersion-shifted fiber," *IEEE Photon. Technol. Lett.*, vol. 16, no. 11, pp. 2520–2522, Nov. 2004.

Michael Galili was born in Aabenraa, Denmark, in 1977. He received the M.Eng. in applied physics in 2003 from the Technical University of Denmark, Lyngby, Denmark, and the Ph.D. degree in optical communications and signal processing from the Communications Optics and Materials (COM) Department, Technical University of Denmark in 2007.

He is currently a Postdoctoral Researcher at the Technical University of Denmark. He is the author or coauthor of more than 30 peer reviewed scientific publications. His current research interests include optical signal processing of high-speed optical data signals.

Leif Katsuo Oxenløwe received the B.Sc. degree in physics and astronomy from Niels Bohr Institute, University of Copenhagen, Copenhagen, Denmark in 1996, the International Diploma of Imperial College of Science, Technology and Medicine, London, U.K., in 1998, the M.Sc. degree in physics from the University of Copenhagen, in 1998, and the Ph.D. degree in optical communications from the Technical University of Denmark, Lyngby, Denmark, in 2002.

He is currently an Associate Professor in the Systems Competence Area, Research Center Communications Optics and Materials (COM) Department, Technical University of Denmark, where he is engaged in the experimental research in the field of ultrafast optical communications (above 160 Gb/s). He has been working within the European Union (EU) Information Society Technologies (IST) Project Terabit/s Optical Transmission Systems based on Ultra-high Channel Bitrate (TOPRATE), and has also been involved in the Danish Research Council financed project Semiconductor Components for Optical Signal Processing (SCOOP). From May 2004, he joined and managed the Project Ultranet (ultrahigh-speed data rates for future generation Internet) funded by the Danish Research Council. Since August 2007, he has been engaged in the project NANO-COM funded by the Danish Research Council.

Hans Christian Hansen Mulvad was born in Copenhagen, Denmark, in 1976. He received the M.Sc. degree in physics from the University of Copenhagen, Copenhagen, Denmark, in 2004. He is currently working toward the Ph.D. degree in the Department of Communications, Optics and Materials, Technical University of Denmark, Lyngby, Denmark.

He is currently involved in research on fiber nonlinearities for high-speed signal processing.

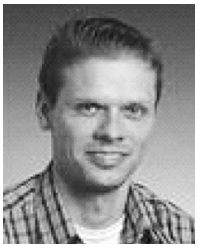

Anders Thomas Clausen was born in Copenhagen, Denmark, in 1967. He received the M.Sc. degree in electrical engineering from the former Electromagnetics Institute (EMI), Danmarks Tekniske Universitet (DTU), Lyngby, Denmark, in 1997, and the Ph.D. degree from the Department of Optics, Communications and Materials (COM), DTU, in 2007.

From 1995 to 1996, he carried out his military service. In 1997, he joined the EMI as a Research Associate, where he was engaged in optical signal processing. He was participating in a number of European Projects, such as HIGHWAY, REPEAT, and METEOR, and also in national projects. In 2001, he was appointed the Group Leader of an Optical Time-Division Multiplexing (OTDM) Group, COM, where he is currently a Postdoctoral Researcher. He is the author or coauthor of more than 100 peer reviewed scientific publications. His current research interests include ultrahigh-speed signal processing at bit rates of 160 Gb/s and beyond.

Palle Jeppesen (M'69) was born in Vordingborg, Denmark, in 1941. He received the Graduate degree in January 1967, the M.Sc. degree in electrophysics, and the Lic. Techn. (Ph.D.) and Dr. Techn. (D.Sc.) degrees in microwave solid state in 1970 and 1978, respectively, all degrees from the Technical University of Denmark (DTU), Lyngby, Denmark.

From 1968 to 1969, he was a Research Associate at Cornell University, Ithaca, NY, and from 1969 to 1970, a Project Engineer at Cayuga Associates, Ithaca, where at both places, he was engaged in the field of GaAs Gunn effect microwave oscillators. From 1970 to 1998, he was an Assistant, Associate, Research, and a Full Professor at the Department of Electromagnetic Systems (EMI), DTU, first in microwave electronics, and since 1974, in optical communications. At EMI, he was the Head of the Optogroup from 1974 to 1988, and the Head of the Center for Broadband Telecommunications from 1988 to 1998. From 1982 to 1984, he was a part-time Manager of R&D at NKT Elektronik, now Draka Denmark Optical Cable, OFS Fitel Denmark, and Tellabs Denmark. Since 1998, he has been a Professor in optical communications at the Research Center, Communications and Materials (COM), DTU, where he is the Head of the Systems Competence Area. His current research interests include optical multilevel modulation formats and 160–640 Gb/s optical communication. He is currently the supervisor for six Ph.D. students.

Prof. Jeppesen has been a member of numerous evaluation committees at DTU and in other countries—in 2002 for Styrelsen för Strategisk Forskning, in 2003 and 2004 for Vetenskapsrådet and for Chalmers Tekniska Högskolan in Sweden, and in 2007, the peer review panel for European Research Council Starting Grants and again for Styrelsen för Strategisk Forskning in Sweden. He was the recipient of the P. Gorm Petersens Memorial Stipend in 1974, the Esso Prize in 1978, the Villum Kann Rasmussen Prize in 1988, and the Alexander Foss Gold Medal in 2005.